

Physics issues of compact drift optimized stellarators

D.A. Spong, S.P. Hirshman, L.A. Berry, J.F. Lyon, R.H. Fowler,
D.J. Strickler, M.J. Cole, B.N. Nelson, D.E. Williamson
Oak Ridge National Laboratory,
Oak Ridge, Tennessee, United States of America

A.S. Ware, D. Alban
University of Montana,
Missoula, Montana, United States of America

R. Sánchez
Universidad Carlos III de Madrid,
Madrid, Spain

G.Y. Fu, D.A. Monticello
Princeton Plasma Physics Laboratory, Princeton University,
Princeton, New Jersey, United States of America

W.H. Miner, P.M. Valanju
University of Texas,
Austin, Texas, United States of America

Abstract. Physics issues are discussed for compact stellarator configurations which achieve good confinement by the fact that the magnetic field modulus $|B|$ in magnetic co-ordinates is dominated by poloidally symmetric components. Two distinct configuration types are considered: (1) those which achieve their drift optimization and rotational transform at low β and low bootstrap current by appropriate plasma shaping; and (2) those which have a greater reliance on plasma β and bootstrap currents for supplying the transform and obtaining quasi-poloidal symmetry. Stability analysis of the latter group of devices against ballooning, kink and vertical displacement modes has indicated that stable β values on the order of 15% are possible. The first class of devices is being considered for a low β near term experiment that could explore some of the confinement features of the high β configurations.

1. Introduction

Stellarator optimization techniques have allowed the exploration of design parameters corresponding to compact (aspect ratios in the range $R_0/\langle a \rangle = 2.5-4$), low field period ($N_{fp} = 2-4$) toroidal devices with attractive physics properties. These configurations permit lower cost near term experiments with the same plasma minor radius $\langle a \rangle$ as the more conventional large aspect ratio stellarator approach. In addition, they offer the longer term potential of a more economically sized, higher power density fusion reactor. These devices will also explore new regimes of stellarator parameter space where the transport physics, equilibrium resilience, plasma flow dynamics, RF heating strategies and microturbulence are expected to be quite different than at higher aspect ratios. The strong geometric couplings which occur at lower aspect ratios generally require a numerical approach and present challenging computational

problems owing to the broad spectra of $|B|$ (in Fourier space) which must be considered. We have utilized a transport optimization strategy based on quasi-omnigeneity (QO) [1, 2] that minimizes particle drifts by targeting both the variation of the longitudinal adiabatic invariant J within magnetic flux surfaces and local neoclassical transport rates as calculated by the DKES [3] code. Additional optimization targets are Mercier stability, ballooning stability based on the COBRA [4, 5] code, a self-consistent bootstrap current that is reduced (by factors of >3) from that in a tokamak and rotational transform profiles that avoid major resonances.

Previously [2] we analysed 3 and 4 field period QO configurations which were close to quasi-helically symmetrical states for aspect ratios in the range $R_0/\langle a \rangle = 3.5-4$. In this article, we focus on 2 and 3 field period devices that are close to quasi-poloidally symmetrical states for aspect ratios in the range $R_0/\langle a \rangle = 2.5-3.5$. The emergence of this

form of quasi-symmetry has been a natural outcome of directing our QO optimization approach towards lower field periods and lower aspect ratio. Improvements of collisionless particle confinement resulting from the introduction of poloidally symmetric bumpy fields have previously been analysed for the case of helical axis heliotron devices [6]. Quasi-poloidal symmetry also offers the unique property of minimizing the viscous damping (i.e. as caused by magnetic pumping) in the direction of the $E_r \times B$ drift. This feature may be of importance in accessing enhanced confinement regimes which depend on $E_r \times B$ shear and should lead to much lower parallel flows than in quasi-axisymmetric devices [7]. Two configuration choices have emerged from our optimization studies. The first type, which we regard as more appropriate for a near term experiment, relies on plasma shaping to achieve most of its rotational transform and quasi-poloidal symmetry. The second type, which we regard as a longer term option owing to its more challenging startup and heating requirements, derives most of its transform and quasi-symmetry from the finite plasma $\langle\beta\rangle$ driven bootstrap currents. In this respect it resembles an advanced tokamak, but because of its quasi-poloidal symmetry the bootstrap current is spatially well aligned and is lower (by a factor of 3 or 4) than the equivalent tokamak. This latter feature leads to higher $\langle\beta\rangle$ stability towards external kink and vertical modes than in the advanced tokamak.

2. Low $\langle\beta\rangle$, near term experimental configuration

In Fig. 1 we show the flux surface shapes and coils for a 2 field period, $R_0/\langle a\rangle = 2.5$ device which is of the first type mentioned above.

The rotational transform profiles with and without bootstrap current and the Fourier coefficients B_{mn} of $|B|$ are shown in Figs 2(a) and (b). As previously indicated, these devices are dominantly quasi-poloidal (i.e. the $m = 0$ components: (0,0), (0,1) and (0,2) of B_{mn} are the largest) and have most of their rotational transform provided through the external coils. The bootstrap current flows in the direction which increases the transform; this fact, coupled with the positive shear in the transform, provides stabilization against neoclassical tearing instabilities. Thresholds for ballooning instabilities are currently found to be $\langle\beta\rangle = 1.8\text{--}2\%$ (in this article angle brackets around variables represent volume averages). We have used pressure profiles with zero gradient at the plasma edge so as not to drive finite bootstrap currents at the edge; such edge currents are not thought to be maintainable but can lead, in some cases, to higher ballooning thresholds (although the kink mode should be destabilized). The predicted bootstrap current levels (in the low collisionality limit) for this device are about 1/3 of those in the equivalent tokamak configuration. For example, in a $\langle B\rangle = 1$ T,

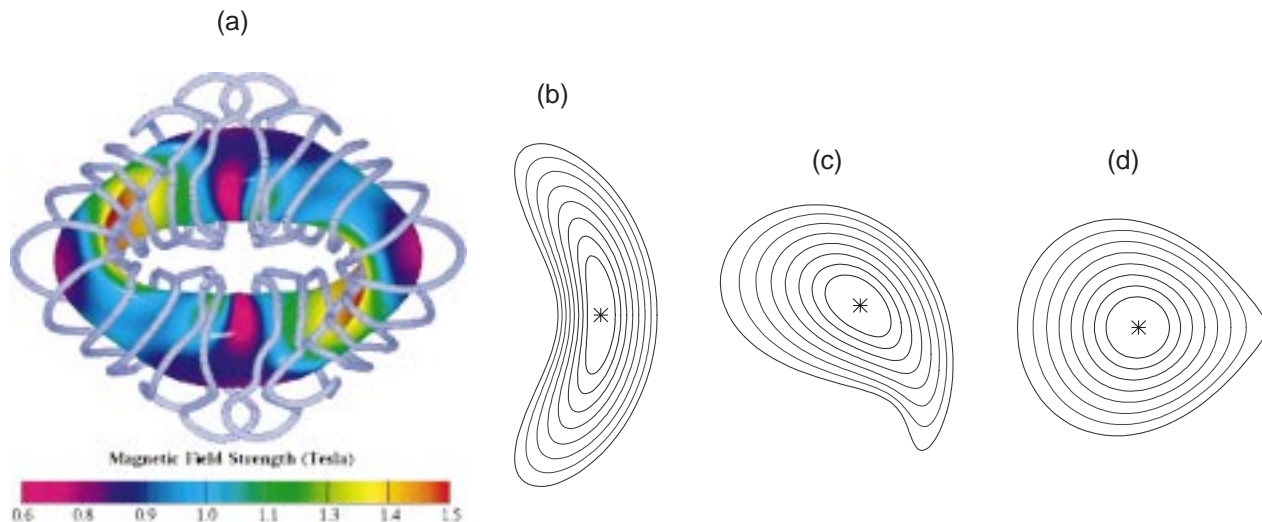


Figure 1. (a) Top view of the outer flux surface and modular coils (in blue) for an $N_{fp} = 2$, $R_0/\langle a\rangle = 2.5$ device; (b, c, d) VMEC flux surfaces at toroidal angles $\zeta/N_{fp} = 0^\circ$, 90° and 180° .

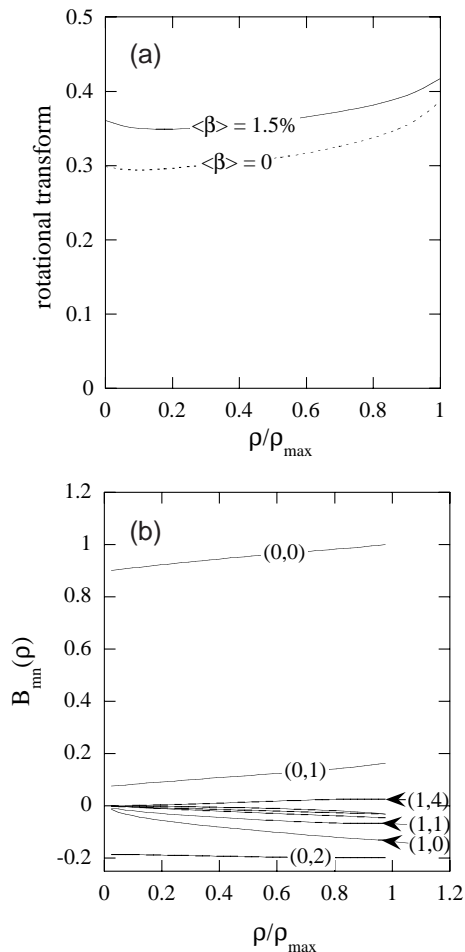


Figure 2. (a) Rotational transform profiles, and (b) B_{mn} amplitudes versus toroidal flux. The poloidal and toroidal mode numbers (m, n) are indicated for the larger components of B_{mn} .

$R_0 = 0.8$ m device at $\langle\beta\rangle = 1.5\%$, 34 kA of bootstrap current would flow, on the basis of the low collisionality limit. Calculations of bootstrap current for collisionalities representative of experimental conditions (Table 1) are under way using the DKES model [3]; preliminary results indicate that the bootstrap current will be reduced (by $\sim 1/3$) from the low collisionality limit and will depend weakly on the value of the ambipolar electric field.

Our analysis of neoclassical transport in this device has been directed at regimes which would be accessible in a $\langle B \rangle = 1$ T, $R_0 = 0.8$ m device with 28 GHz ($B = 0.5$ T) and 53 GHz ($B = 1$ T) ECH sources available. The impact of supplementary ICH (1 MW), which is available in the 40–80 MHz range, has also been considered; this would allow access to higher density regimes than ECH (density

cut-off limited). Our transport analysis has been carried out with the DELTA5D Monte Carlo model, which is a generalization of an earlier stellarator Monte Carlo code [8] to include energetic beam and alpha populations, ICH, global lifetime estimates and bootstrap current options. Populations of ions and electrons are initially distributed randomly in pitch angle and in poloidal and toroidal angles. The radial distribution is consistent with a flat density profile while the energy distribution is modelled after parabolic-squared temperature profiles. As particles leave the outer flux surface boundary, they are replaced with new initial values chosen from the above distributions. We assume an ion root ambipolar potential profile which rises from the centre inversely with the drop-off in electron temperature profile and we take $e\phi/kT_e = 1$ at the plasma edge. Electron root profiles ($e\phi/kT_e < 0$) have also been examined for the ECH cases; however, for the same edge value of $|e\phi/kT_e|$, these cases lead to nearly the same global confinement times as the ion root. We are also developing a self-consistent calculation of the electric field using the DKES model [3] similar to work that has been carried out [9] in modelling the W7-AS experiment. Initial results from these calculations near the plasma edge show ion root behaviour with $e\phi/kT_e \approx 1$. Table 1 lists the parameters we have considered for the various heating scenarios (here we assume $Z_{eff} = 1$).

Applying the Monte Carlo transport model to the above parameters leads to the predicted neoclassical lifetimes in column 6 in the table, labelled $\tau_{E,global}$ (here $\tau_{E,global}$ is the overall neoclassical energy lifetime, taking into account both $\tau_{E,ion}$ and $\tau_{E,elec}$); in the final column the ISS95 [10] empirical stellarator confinement scaling, assuming no enhancement factor, is given for comparison. As can be seen, the neoclassical loss rates are considerably smaller than the ISS95 [10] rates, especially at the higher range of densities that can be accessed with ICRF heating.

Free boundary and field line following calculations have also been carried out on the basis of the modular coil set shown in Fig. 1 in order to check that a good reconstruction of flux surfaces is obtained and that neoclassical confinement is preserved. Comparisons of Monte Carlo energy lifetimes based on free boundary equilibria show less than 10% change from the original fixed boundary results. Also, this configuration has been analysed with the PIES [11] code up to $\langle\beta\rangle = 1.6\%$, indicating that only a minimal loss of flux surfaces occurs over the outer 10% of the plasma radius.

Table 1. Plasma parameters and predicted neoclassical lifetimes for a $\langle B \rangle = 0.5\text{--}1$ T, $R_0 = 0.83$ m, $N_{fp} = 2$ device, based on ISS95 scaling with enhancement factor $H = 1$

Heating, magnetic field	Density (10^{20} m $^{-3}$)	T_e, T_i (keV)	ν_{*e}, ν_{*i}	$\langle \beta \rangle$ (%)	$\tau_{E,global}$ (ms)	$\tau_{E,ISS95}$ (ms)
0.5 MW ECH, $B = 1$ T	0.18	1.4, 0.15	0.02, 1.6	0.7	10.2	8.1
1 MW ECH, $B = 0.5$ T	0.045	2.1, 0.2	0.002, 0.22	1	2.1	1.5
1 MW ICH, $B = 1.0$ T	0.83	0.5, 0.5	0.68, 0.64	2	71.7	11.7
1 MW ICH, $B = 0.5$ T	0.59	0.4, 0.25	0.75, 1.8	3.7	16.4	5.5

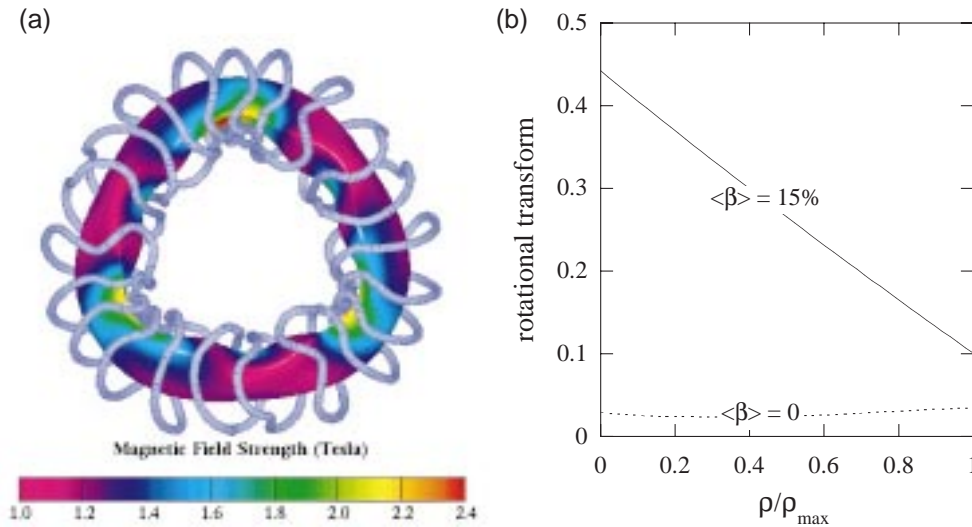


Figure 3. (a) Top view of the outer flux surface with modular coils (in blue) for an $N_{fp} = 3$, $R_0/\langle a \rangle = 3.7$ device; (b) rotational transform profiles with and without bootstrap current.

3. High $\langle \beta \rangle$ configurations

In addition to the device described in Section 2, we have also found nearly quasi-poloidal 2 and 3 field period configurations ($R_0/\langle a \rangle = 2.7\text{--}3.7$) in which the plasma bootstrap current supplies a large fraction of the transform. In the case of 3 field periods, these devices fully access the second regime for ballooning stability at around $\langle \beta \rangle > 15\%$ with second regime stabilization entering in from the outer region of the plasma at $\langle \beta \rangle = 6\text{--}7\%$. Configurations with 2 field periods have also been found which achieve second regime stabilization for $\langle \beta \rangle$ as low as 1%. Vertical and external kink modes are weakly unstable at $\langle \beta \rangle = 15\%$ and can be stabilized by a very small reduction (10%) of the self-consistent bootstrap current. However, these modes are sufficiently

near marginal stability that a slight modification in the 3-D shape should also provide stabilization. An example of a 3 field period configuration of this type is shown in Fig. 3 along with its transform profile with and without plasma bootstrap currents.

At this relatively low value of ι , the collisionless bootstrap current in this device is about 1/4 of that in the equivalent tokamak. These configurations have tokamak-like transform profiles and approach quasi-poloidal symmetry with increasing $\langle \beta \rangle$. This feature is evident in the B_{mn} spectrum shown in Fig. 4(a), where the $n = 0$ ((0,0), (0,1) and (0,2)) components of B_{mn} may be seen to dominate.

At such high values of $\langle \beta \rangle$, the $|B|$ contours also become poloidally closed (at fixed toroidal cross-sections) and begin to align with flux surfaces. This is a further indication of the enhancement in

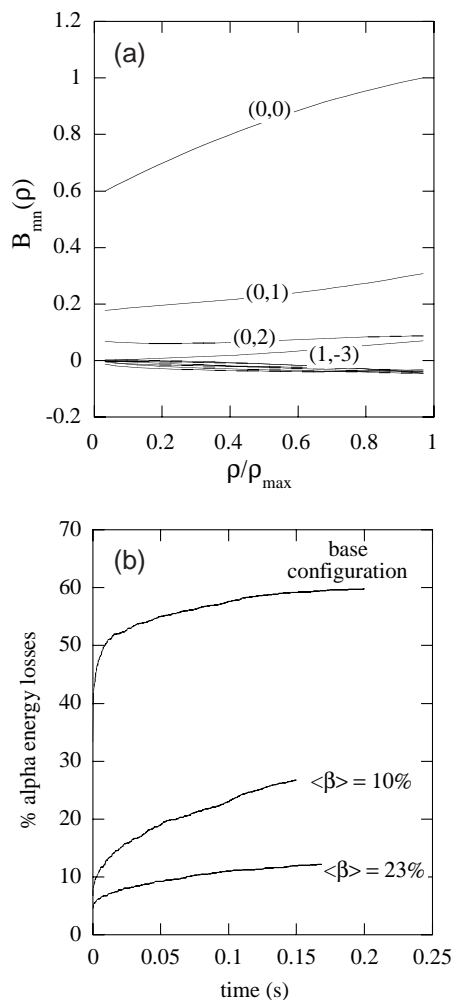


Figure 4. (a) B_{mn} amplitudes versus toroidal flux for a $\langle\beta\rangle = 23\%$, $N_{fp} = 3$ device; (b) fraction of 3.5 MeV alpha particle losses for a reactor scale version ($R_0 = 10$ m, $\langle B \rangle = 5$ T) with increasing $\langle\beta\rangle$.

quasi-poloidal symmetry associated with increasing $\langle\beta\rangle$. As may be seen from Fig. 4(a), the $B_{0,0}$ component is depressed in the centre; this is a result of the diamagnetic well (shift due to Pfirsch–Schlüter currents) at this value of $\langle\beta\rangle$. The poloidal gradient B drifts associated with this radial variation in $B_{0,0}$ are helpful for the confinement of energetic particles, as is shown in the study of alpha confinement in Fig. 4(b). Here the curve labelled as the base configuration is constrained to have the same outer flux surface shape and transform profile as the $\langle\beta\rangle = 23\%$ case but does not include the plasma diamagnetic current effects which lead to the modified B_{mn} spectrum shown in Fig. 4(a) (i.e. this is essentially a $\langle\beta\rangle = 0$ case, except that an ad hoc plasma current is provided which is equal to the bootstrap current

of the $\langle\beta\rangle = 23\%$ case). The level of alpha energy losses ($\sim 12\%$) at the highest $\langle\beta\rangle$ are the lowest we have found in modelling any of this class of compact stellarator devices.

4. Conclusions

We have found attractive compact stellarators with 2 and 3 field periods and aspect ratios in the range $R_0/\langle a \rangle = 2.5$ – 3.5 which maintain good neo-classical confinement by approaching quasi-poloidal symmetry. These configurations can be produced by relatively simple modular magnet coils from which we have verified flux surface reconstruction and which retain the confinement properties of the original fixed boundary equilibrium. Two classes of this type of compact stellarator have been examined: one which produces most of the rotational transform and quasi-poloidal symmetry through external means and a second which relies more on the plasma currents associated with high plasma $\langle\beta\rangle$ to produce these effects. We envision the first type of configuration to be a candidate for a near term experiment with $B \approx 1$ T and $R_0 \approx 1$ m. Our transport analysis has shown that such a device has an adequate margin of confinement above ISS95 scaling (up to 6 times ISS95). The second type of device, which may form the basis for a reactor version of a compact QO stellarator, is computed to achieve very high $\langle\beta\rangle$ limits ($\sim 15\%$) for a low aspect ratio stellarator and very good (tokamak-like) energetic alpha particle confinement.

Acknowledgement

This research was sponsored by the Office of Fusion Energy of the US Department of Energy under contract DE-ACO5-96OR22464.

References

- [1] Hirshman, S.P., et al., Phys. Plasmas **6** (1999) 1858.
- [2] Spong, D.A., et al., Nucl. Fusion **40** (2000) 563.
- [3] Van Rij, W.I., Hirshman, S.P., Phys. Fluids B **1** (1989) 563.
- [4] Sanchez, R., Hirshman, S.P., Whitson, J.C., Ware, A.S., J. Comput. Phys. **161** (2000) 576.
- [5] Sanchez, R., Hirshman, S.P., Ware, A.S., Berry, L.A., Spong, D.A., Plasma Phys. Control. Fusion **42** (2000) 641.
- [6] Yokohama, M., et al., Nucl. Fusion **40** (2000) 261.
- [7] Nielson, G.H., et al., Phys. Plasmas **7** (2000) 1911.

- [8] Fowler, R.H., Rome, J.A., Lyon, J.F., Phys. Fluids **28** (1985) 338.
- [9] Baldzuhn, J., Kick, M., Maassberg, H., W7-AS Team, Plasma Phys. Control. Fusion **40** (1998) 967.
- [10] Stroth, U., et al., Nucl. Fusion **36** (1996) 1063.
- [11] Reiman, A., Greenside, H., J. Comput. Phys. **75** (1988) 1423.

(Manuscript received 7 October 2000

Final manuscript accepted 2 February 2001)

E-mail address of D.A. Spong: spongda@ornl.gov

Subject classification: B0, St; B0, Sd; F0, St; F0, Sd